

Strength of the Vortex-Pinning Interaction from Real-Time Dynamics

Aurel Bulgac,¹ Michael McNeil Forbes,^{2,3} and Rishi Sharma⁴

¹*Department of Physics, University of Washington, Seattle, Washington 98195–1560 USA*

²*Institute for Nuclear Theory, University of Washington, Seattle, Washington 98195–1550 USA*

³*Department of Physics, University of Washington, Seattle, Washington 98195–1560 USA*

⁴*TRIUMF, Vancouver, British Columbia, V6T2A, Canada*

(Dated: June 9, 2021)

We present an efficient and general method to compute vortex-pinning interactions – which arise in neutron stars, superconductors, and trapped cold atoms – at arbitrary separations using real-time dynamics. This method overcomes uncertainties associated with matter redistribution by the vortex position and the related choice of ensemble that plague the typical approach of comparing energy differences between stationary pinned and unpinned configurations: uncertainties that prevent agreement in the literature on the sign and magnitude of the vortex-nucleus interaction in the crust of neutron stars. We demonstrate and validate the method with Gross-Pitaevskii-like equations for the unitary Fermi gas, and demonstrate how the technique of adiabatic state preparation with time-dependent simulation can be used to calculate vortex-pinning interactions in fermionic systems such as the vortex-nucleus interaction in the crust of neutron stars.

PACS numbers: 97.60.Jd 26.60.-c 26.60.Gj 21.60.-n

arXiv:1302.2172v2 [nucl-th] 14 Nov 2013

VORTEX-PINNING INTERACTIONS play an important role in the dynamics of various condensed superfluid systems such as superconductors [1], trapped cold-atom gases [2], and possibly neutron stars [3], where the angular momentum carried by vortices can have an observable impact. For example, pulsar glitches – sudden increases in the rotation frequencies of neutron stars – are theorized [4] to arise from a sudden macroscopic unpinning of vortices. In equilibrium, the superfluid and nonsuperfluid components of a pulsar rotate at the same angular frequency. The pulsar loses angular momentum through magnetic radiation, and the crust slows down gradually, reducing the pulsation rate. To maintain equilibrium, the superfluid must also release angular momentum by diluting the vortex concentration, but the presence of pinning sites (nuclei, lattice sites, defects, etc.) may arrest the vortex motion; stress would build until a large number of vortices rapidly unpin, dilute, and transfer their angular momentum to the crust, rapidly increasing in the pulsation rate – the glitch.

Despite almost 40 years, the feasibility of this mechanism is still poorly understood. The conventional picture has the angular momentum stored by the neutron superfluid in the crust, with pinning provided by nuclei held in a lattice by the electrostatic (Coulomb) interaction. (Dilute neutron matter is well approximated [5] by the same unitary Fermi gas (UFG) produced in cold-atom experiments [6].) Pinning may also occur on flux tubes [7] or due to vortex tangles [8]. Recent results suggest that the crustal neutrons may not support enough angular momentum to explain observed pulsar glitches [9], in which case the interaction between neutron superfluid vortices and proton flux tubes in the outer core [10] or quark matter phases in the core may play a role [11]. In

either case, a reliable technique for calculating vortex-pinning interactions is key. Here we present a dynamical method for determining the sign and strength of vortex-pinning forces in superfluids, and demonstrate that this method can be directly applied to unambiguously calculate the vortex-nucleus interaction using time-dependent density functional theory (TDDFT) for nuclear matter.

Because of the importance of pinning on glitch phenomenology, several attempts have been made to calculate the pinning force in nuclear matter from underlying microscopic models. The earliest calculations used the condensation energy to estimate the pinning force [4, 12]. In Refs. [13], the Ginzburg-Landau (GL) framework was used to give a detailed picture of the (un)pinning process: their calculation includes an estimate of the energy as a function of displacement allowing for an estimate of the pinning force. The next advance was the use of a local density approximation [14] with Wigner-Seitz cells and Gogny [15] and Argonne [16] interactions, which gives a similar density-dependant pattern of (un)pinning as [13] but smaller by almost an order of magnitude.

Unlike vortices in weakly coupled BCS superfluids, vortices in dilute neutron matter (and the UFG) displace a substantial amount of matter from their core [17]. Therefore, comparing “energies” of stationary configurations with a nucleus on the core of a vortex and a nucleus away from the vortex is confounded by a choice of ensemble: should one fix the number of neutrons or the chemical potential in a finite simulation volume?

Computing stationary configurations is also computationally expensive – especially given the high degree of precision required to render meaningful energy differences – and simulations to date have required a high degree of symmetry. For example, recent self-consistent cal-

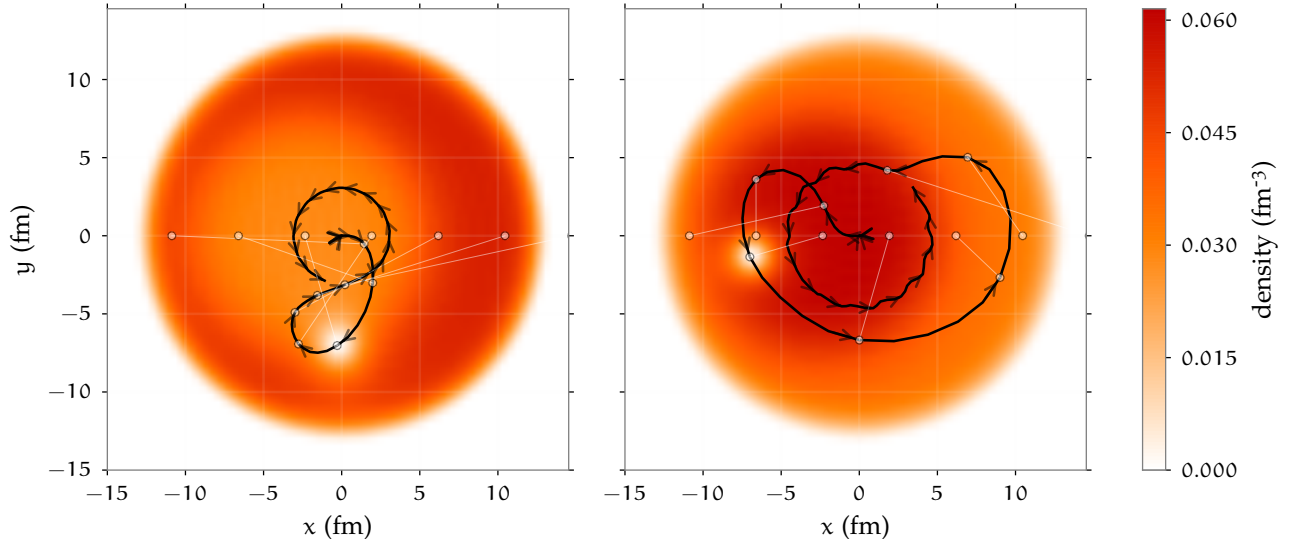


Figure 1. (colour online) Deflection of a vortex in the ETF model of trapped dilute neutron matter as a UFG by a repulsive (left panel) and attractive (right panel) pinning potential $V_{\text{pin}}(r) = \pm 3.5 \text{ MeV} / [1 + \exp(r/\text{fm} - 7.5)]$ moving on a straight line from left to right at a constant subsonic velocity $v \approx 0.1c_s$. The trajectory of the vortex is shown by the (black) curve and the relative separation vector between the pinning site, and the vortex core is shown as thin (white) lines for select times connecting the corresponding dots on the trajectories. Initially the potential displaces the bulk superfluid, carrying the vortex to the right/left. Once the potential overlaps with the vortex, the vortex rapidly moves down/up – (almost) perpendicular to the force. In the frame shown on the left, the pinning site is just to the left of the centre ($x \approx -2.5 \text{ fm}$) and the vortex is moving (almost) perpendicular along the edge of the pinning potential. After the potential has passed through, the vortex orbits in a counterclockwise circle direction due to boundary effects from the trap that can be quantitatively described in this sharp, flat trap by placing an image vortex outside of the potential to cancel the tangential current at the boundary: this induces a counterclockwise superflow v_s in Eq. (1). The geometry of the right simulation is such that the potential carries the vortex around almost the entire trap: This extended interaction allows the pinning potential to excite phonons in the system visible as ripples in the circular trajectory.

culations [18–20] using Hartree-Fock-Bogoliubov (HFB) functionals extract the pinning energy of a vortex on a single nucleus using a cylindrical geometry. In particular, the conclusion of [19] that the pinning force is repulsive (glitches would thereby require interstitial pinning) was questioned by [21] but addressed in [20], while a different set of calculations using the local density approximation suggests that pinning is attractive over a substantial region in the inner crust [18, 22]. Moreover, nearby vortices and the Casimir effect can significantly polarize a nucleus – an effect absent in simple cylindrical geometries – dramatically changing the nature of the nuclear pinning sites and disrupting the regularity of the nuclear lattice [23].

Characterizing the nuclear-pinning interaction will thus require fully 3D (unconstrained by symmetries) self-consistent calculations using realistic nuclear functionals. Highly accurate asymmetric stationary states in full 3D are currently not feasible (these require a full diagonalization of the single-particle Hamiltonian), but TDDFT algorithms can be applied to the unconstrained 3D problem (which requires only applying the Hamiltonian), and scale well to massively parallel supercomputers for both cold atoms and nuclei, as has been demonstrated

in [24]. We now present a qualitatively new approach for calculating vortex-pinning interactions, unencumbered by the aforementioned issues, utilizing only real-time dynamics.

The idea, similar to the Stern-Gerlach experiment, is to observe how a vortex moves when approached by a nucleus. To zeroth order, the sign of the interaction is determined qualitatively by the direction of the motion (Fig. 1); with a more careful inspection, one can extract the force-separation relationship $F(r)$ (Fig. 2).

We validate our procedure using a dynamical extended Thomas-Fermi (ETF) model [25–28], equivalent to a Gross-Pitaevskii equation (GPE) for bosonic “dimers” $m_B = 2m$ of fermionic pairs, with an equation of state $\mathcal{E}(n) \propto \xi \rho^{5/3}$ characterized by the Bertsch parameter $\xi \approx 0.37$ tuned to consistently fit both quantum Monte Carlo (QMC) and experimental results [27]. Despite the computational simplicity of the ETF model, it has been demonstrated to quantitatively reproduce a range of low-energy dynamics of both UFG experiments [26] and fermionic density functional theory (DFT) simulations [28]. The UFG should also qualitatively model the dilute neutron superfluid in the crust of neutron stars [5] due to the large neutron-neutron scattering

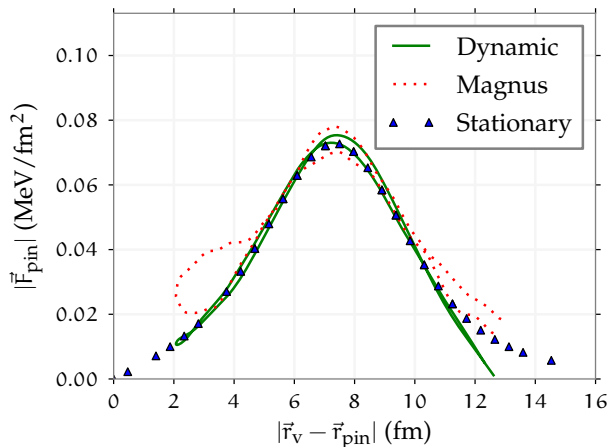


Figure 2. (color online) Here we demonstrate consistency in dynamically extracting a vortex-pinning force. We use the nuclear pairing potential [15] $V_{\text{pin}}(r) = 0.75 \text{ MeV}/[1 + \exp(r/\text{fm} - 7.5)]$ at densities $\rho \sim 0.045 \text{ fm}^{-3} \approx 0.28\rho_{\text{sat}}$. The triangular (blue) points come from the computationally expensive “stationary” method, while the solid (green) curve comes from using the “dynamic” real-time evolution analogous to that shown on the left panel of Fig. 1. The dotted (red) curve shows the Magnus estimate for the force (1) using a Thomas-Fermi approximation for ρ_s and estimating \vec{v}_s from the image vortex [30]. The double curves come from the pinning site moving in then out.

length $a_{nn} \approx -18.9 \text{ fm}$ [29]. Thus, by using a physically motivated model of the nuclear pairing potential [15], we anticipate that these ETF calculations will provide a fairly good approximation of future fermionic TDDFT simulations.

To gain some intuition for the vortex-nucleus interaction, consider the phenomenological Hall-Vinen-Iordanskii (HVI) equation (see [31] for a discussion) for a vortex in 2D:

$$M\ddot{\vec{r}}_v - \vec{f}_{\text{qp}} = \rho_s \vec{\kappa} \times (\dot{\vec{r}}_v - \vec{v}_s) + \vec{F}_v. \quad (1)$$

Here, \vec{r}_v is the position of the vortex, the force \vec{F}_v is per unit length along the vortex, ρ_s is the number density of the “background” superfluid, $\vec{\kappa} = 2\pi\hbar\hat{z}$ is the quantized vortex circulation, and \vec{v}_s is the “background” superfluid velocity. This equation should only be taken as an intuitive guide since terms on the left-hand side are ill-defined. The “mass of the vortex” M , for example, depends strongly on the way it is measured [32], and the force \vec{f}_{qp} due to excited phonons has significant memory effects.

For slowly accelerating vortices, the contribution from the term proportional to $\ddot{\vec{r}}_v$ is small. Furthermore, if the vortex and pinning site move sufficiently slowly, phonons are not excited ($\vec{f}_{\text{qp}} = 0$), and we can ignore the entire left-hand side of Eq. (1) [33]. This leaves the well-

established Magnus relationship $\rho_s \vec{\kappa} \times (\dot{\vec{r}}_v - \vec{v}_s) \approx -\vec{F}_v$ relating the force \vec{F}_v applied to the vortex and its perpendicular velocity $\dot{\vec{r}}_v$ relative to the background superfluid velocity \vec{v}_s . Thus, by observing the dynamical deflection of a vortex from a nuclear pinning site, one can directly extract the direction and approximate magnitude of the vortex-nucleus force without requiring a subtle subtraction of energies.

In small systems, the Magnus relation can only be used to estimate the magnitude of the force since the superfluid density ρ_s and velocity v_s are not precisely defined, though reasonable estimates can be obtained. With an external pinning potential $V_{\text{pin}}(\vec{r}_{\text{pin}} - \vec{x})$, however, one can directly and unambiguously calculate the force on the pinning site:

$$\vec{F}_{\text{pin}} = - \int d^3x \frac{\partial V_{\text{pin}}(\vec{r}_{\text{pin}} - \vec{x})}{\partial \vec{r}_{\text{pin}}} \rho(\vec{x}). \quad (2)$$

In the nuclear context where neutrons are present in the both the pinning site (the nucleus) and the superfluid medium, the force can be obtained in two ways: 1) Eq. (2) can be directly applied to a Coulomb potential (V_{pin}) that couples to the proton charge density (ρ) – this will be the force that the vortex exerts on the nuclear lattice – or, 2) one can estimate the force using Newton’s law $\vec{F}_{\text{pin}} = m_{\text{pin}}\vec{a}_{\text{pin}}$ for a dynamic pinning site comprising protons and entrained neutrons. The position of the pinning site can be unambiguously defined as the center of mass (CM) of the protons, and the effective mass m_{pin} can be estimated [34].

What remains is to prepare the initial conditions with a vortex and nucleus interacting at various distances. The traditional self-consistent approach requires diagonalizing $N \times N$ matrices ($N = N_x N_y N_z$) which takes $\mathcal{O}(N^3)$ operations. This is not feasible for realistic $N \sim 10^6$, as *each iteration* would required a day of supercomputing wall time. Instead, one can use adiabatic state preparation [35, 36] which takes $\mathcal{O}(N^2 \log N)$ operations. The idea is to adiabatically evolve in real time a state of some solvable system to a desired initial state in the system of interest. For example, starting with a noninteracting (Bose) gas trapped in a harmonic potential $V_{\text{HO}}(r) = m_B \omega^2 r^2/2$, we can form either the ground state $\Psi_{\text{GS}} \propto \exp(-m_B \omega r^2/2)$, or an exact vortex “Landau level” $\Psi_\delta \propto (x + iy - \delta) \exp(-m_B \omega r^2/2\hbar)$ (stationary in a rotating frame) with angular momentum $l_z = N\hbar/(1 + m_B \omega \delta^2/\hbar)$ where δ is the displacement of the vortex node from the centre of the harmonic trap. From this exact noninteracting state we adiabatically evolve the system to an interacting state in the desired trapping potential V_{trap} by simultaneously switching on the interaction $s\xi$ and interpolating the trapping potentials $V_t = (1 - s)V_{\text{HO}} + sV_{\text{trap}}$ where $s = s(t/T)$ is a smooth C^∞ switching function that goes from 0 to 1

over a characteristic time T chosen to be longer than any intrinsic time scale in the system:

$$s\left(\frac{t}{T}\right) = \frac{1}{2} + \frac{1}{2} \tanh\left[\alpha \tan\left(\frac{\pi t}{T} - \frac{\pi}{2}\right)\right] = \text{---} \quad (3)$$

From Ψ_{GS} we can generate the ground state, and from $\Psi_{\delta=0}$ we can generate a single vortex in the centre of the trap, both to high precision. The adiabatic state preparation can be significantly accelerated by introducing a ‘‘quantum friction’’ term to remove phonon noise [36]. With this combined approach, one can efficiently produce almost any desired initial state with less than a day of supercomputing wall time.

To accurately measure the vortex-pinning interaction, one can choose as a final potential $V_T = V_{\text{trap}} + V_{\text{pin}}$: an axially symmetric trap of suitably flat bottom and a pinning potential in the center. By generating a configuration with a vortex orbiting in a circle at radius r , we can use Eq. (2) to calculate the force exerted on the centrally located pinning potential: axial symmetry ensures that this is precisely the vortex-pinning force at separation r . We use this procedure within the ETF model to accurately calculate the ‘‘stationary’’ (in a rotating frame) vortex-pinning interaction shown in Fig. 2.

The present demonstration has been limited to quasi-2D simulations. The procedure will work just as well in fully 3D simulations. New effects such as the bending of a vortex line when approached by a pinning site can just as easily be analyzed: the vortex line will either be repelled by the pinning site – bowing out to avoid it – or will be sucked in. We have considered here only moving the pinning site, but one could also consider manipulating parts of the vortex with pinning potentials, dragging the pinned vortex along a trajectory instead. In simulations with realistic nuclei, the vortex-nucleus interaction will also excite and deform the nucleus – significantly affecting the vortex-nucleus interaction. It is conceivable also that a vortex lines could break and attach to various nuclear defects like rods or plates: the dynamics of such broken vortex lines may also play a important part in explaining neutron star glitches.

We close with a brief analysis of the time evolution. The complex scalar field Ψ obeys an evolution equation of the form

$$i\hbar\Psi = \left(-\frac{\hbar^2\nabla^2}{2m_B} + V_{\text{eff}}[\Psi]\right)\Psi \quad (4)$$

where $V_{\text{eff}}[\Psi]$ is an effective interaction that depends nonlinearly on $|\Psi|$ and on the external trapping and pinning potentials. Consider the quasi-two-dimensional problem where coordinates may be expressed as complex numbers $z = x + iy$: A singly-wound vortex at location z_v may be described by the field $\Psi(z) = (z - z_v)f(z)$, where $f(z)$ is a smooth complex-valued function that we assume

has no roots in the immediate vicinity of the vortex. The evolution equations may then be expressed as follows

$$i\hbar f + \frac{\hbar^2\nabla^2 f}{2m_B} - V_{\text{eff}}[\Psi]f = \frac{i\hbar z_v f - \hbar^2(\partial_x f + i\partial_y f)/m_B}{z - z_v}. \quad (5)$$

The left side is smooth; hence, the pole on the right side must cancel with a root in the numerator, giving us an explicit expression for the vortex velocity

$$\dot{z}_v = [\dot{r}_v]_x + i[\dot{r}_v]_y = \hbar \frac{-i\partial_x f + \partial_y f}{m_B f} \Big|_{z=z_v}. \quad (6)$$

This expression can be written as an exact ‘‘Magnus’’ relation

$$\vec{\kappa} \times (\dot{r}_v - \vec{v}) = \frac{\hbar^2\nabla\rho}{2m_B\rho} \Big|_{z=z_v} \quad (7)$$

where the local ‘‘superfluid velocity’’ \vec{v} is

$$f = \sqrt{\rho}e^{i\phi}, \quad \vec{v} = \vec{\nabla}\phi. \quad (8)$$

The meaning of ρ_s in the HVI equations is not clarified since ρ cancels in Eq. (7). Unfortunately, although \vec{v} is precisely defined and corresponds to \vec{v}_s in some situations, one cannot generally make the correspondence $\vec{v}_s \equiv \vec{v}$. In particular, doing so yields results that differ by as much as 50% in Fig. 2.

The quantities appearing in Eq. (1) are related to long-range momentum transfers and boundary effects, and one must thus be content with reasonable estimates for ρ_s and v_s , for example, from the average behaviours of the relevant quantities near but outside of the vortex core. As Fig. 2 demonstrates, however, the Magnus relation is suitable for extracting the sign and magnitude of the interaction. This also provides an explicit check that the force evaluated using our procedure is what appears on the right side in Eq. (1) governing the vortex dynamics.

Conclusion: We have described how to use time-dependent density functional theory (TDDFT) to efficiently and unambiguously calculate vortex-pinning interactions from real-time dynamical simulations of superfluid systems. We have demonstrated with an extended Thomas-Fermi (ETF) model of the unitary Fermi gas (UFG) that this approach can be applied to calculate the vortex-nucleus interaction using nuclear TDDFTs to model the crust of neutron stars. While we considered only quasi-2D systems here, the size of the problem, the magnitude and accuracy of the force extraction, and the use of pure real-time dynamics ensure that full 3D simulations of realistic fermionic TDDFTs are possible. With available resources [24] one can simulate both finite and infinite nuclear systems in simulation boxes of the order of 80^3 fm^{-3} for up to 10^{-19} s. A resolution to the puzzle

of pulsar glitches will require more than just extracting the vortex-nucleus interaction, but with this real-time method, this crucial step will soon be within reach.

These techniques can also be directly applied to systems of trapped ultracold atoms in a variety of geometries, for example, to explore vortex pinning on optical lattices. In particular, the close approximation of the neutron superfluid by the UFG suggests that cold-atom experiments might also be able to shed light on the glitching puzzle.

We thank S. Reddy and D. Thouless for useful discussions. This material is based upon work supported by the U. S. Department of Energy under Award Numbers DE-FG02-97ER41014 and DE-FG02-00ER41132.

-
- [1] T. Shapoval, V. Metlushko, M. Wolf, B. Holzapfel, V. Neu, and L. Schultz, *Phys. Rev. B* **81**, 092505 (2010), arXiv:0907.2821 [cond-mat.supr-con].
- [2] S. Tung, V. Schweikhard, and E. A. Cornell, *Phys. Rev. Lett.* **97**, 240402 (2006), arXiv:cond-mat/0607697.
- [3] B. Link, R. I. Epstein, and J. M. Lattimer, *Phys. Rev. Lett.* **83**, 3362 (1999), arXiv:astro-ph/9909146.
- [4] P. W. Anderson and N. Itoh, *Nature* **256**, 25 (1975).
- [5] J. Carlson, S. Gandolfi, and A. Gezerlis, *Prog. Theor. Exp. Phys.* **2012**, 01A209 (2012), arXiv:1210.6659 [nucl-th].
- [6] W. Zwerger, ed., *The BCS–BEC Crossover and the Unitary Fermi Gas*, Lecture Notes in Physics, Vol. 836 (Springer-Verlag, Berlin Heidelberg, 2012).
- [7] M. Ruderman, T. Zhu, and K. Chen, *Astrophys. J.* **492**, 267 (1998).
- [8] C. Peralta, A. Melatos, M. Giacobello, and A. Ooi, *Astrophys. J.* **651**, 1079 (2006), arXiv:astro-ph/0607161.
- [9] N. Andersson, K. Glampedakis, W. C. G. Ho, and C. M. Espinoza, *Phys. Rev. Lett.* **109**, 241103 (2012), arXiv:1207.0633; N. Chamel, *Phys. Rev. Lett.* **110**, 011101 (2013), arXiv:1210.8177.
- [10] B. Link, “Observable core response in neutron star spin glitches,” (2012), arXiv:1211.2209 [astro-ph.SR].
- [11] J. A. Bowers and K. Rajagopal, *Phys. Rev. D* **66**, 065002 (2002), arXiv:hep-ph/0204079; M. Mannarelli, K. Rajagopal, and R. Sharma, *ibid.* **76**, 074026 (2007), arXiv:hep-ph/0702021 [hep-ph].
- [12] M. A. Alpar, *Astrophys. J.* **213**, 527 (1977); M. A. Alpar, D. Pines, P. W. Anderson, and J. Shaham, *Astrophys. J.* **276**, 325 (1984).
- [13] R. I. Epstein and G. Baym, *Astrophys. J.* **328**, 680 (1988); B. K. Link and R. I. Epstein, *Astrophys. J.* **373**, 592 (1991).
- [14] P. M. Pizzochero, L. Viverit, and R. A. Broglia, *Phys. Rev. Lett.* **79**, 3347 (1997), arXiv:astro-ph/9709060v1.
- [15] R. A. Broglia, F. De Blasio, G. Lazzari, M. Lazzari, and P. M. Pizzochero, *Phys. Rev. D* **50**, 4781 (1994).
- [16] M. Baldo, J. Cugnon, A. Lejeune, and U. Lombardo, *Nucl. Phys. A* **515**, 409 (1990).
- [17] Y. Yu and A. Bulgac, *Phys. Rev. Lett.* **90**, 161101 (2003), arXiv:nucl-th/0212072.
- [18] P. Donati and P. M. Pizzochero, *Nucl. Phys. A* **742**, 363 (2004).
- [19] P. Avogadro, F. Barranco, R. A. Broglia, and E. Vigezzi, *Phys. Rev. C* **75**, 012805 (2007), arXiv:nucl-th/0602028v1.
- [20] P. Avogadro, F. Barranco, R. A. Broglia, and E. Vigezzi, *Nucl. Phys. A* **811**, 378 (2008), arXiv:0804.1765.
- [21] P. M. Pizzochero, “Pinning and Binding Energies for Vortices in Neutron Stars: Comments on Recent Results,” (2007), arXiv:0711.3393.
- [22] P. Donati and P. M. Pizzochero, *Phys. Rev. Lett.* **90**, 211101 (2003); *Phys. Lett. B* **640**, 74 (2006).
- [23] A. Bulgac and P. Magierski, *Nucl. Phys. A* **683**, 695 (2001), arXiv:astro-ph/0002377; *Nucl. Phys. A* **703**, 892(E) (2002), arXiv:astro-ph/0002377; P. Magierski and P.-H. Heenen, *Phys. Rev. C* **65**, 045804 (2002), arXiv:nucl-th/0112018; P. Magierski, A. Bulgac, and P.-H. Heenen, *Nucl. Phys. A* **719**, C217 (2003), arXiv:nucl-th/0212093.
- [24] A. Bulgac, Y.-L. Luo, P. Magierski, K. J. Roche, and Y. Yu, *Science* **332**, 1288 (2011); I. Stetcu, A. Bulgac, P. Magierski, and K. J. Roche, *Phys. Rev. C* **84**, 051309(R) (2011), arXiv:1108.3064 [nucl-th]; A. Bulgac, Y.-L. Luo, and K. J. Roche, *Phys. Rev. Lett.* **108**, 150401 (2012), arXiv:1108.1779.
- [25] Y. E. Kim and A. L. Zubarev, *Phys. Rev. A* **70**, 033612 (2004), arXiv:cond-mat/0404513.
- [26] L. Salasnich, F. Ancilotto, N. Manini, and F. Toigo, *Laser Phys.* **19**, 636 (2008), arXiv:0810.1704; L. Salasnich and F. Toigo, *Phys. Rev. A* **78**, 053626 (2008), arXiv:0809.1820; *Phys. Rev. A* **82**, 059902(E) (2010), arXiv:0809.1820; L. Salasnich, *Europhys. Lett.* **96**, 40007 (2011), arXiv:1110.0311; *Few-Body Sys.* **54**, 697 (2013), arXiv:1204.1659.
- [27] M. M. Forbes, S. Gandolfi, and A. Gezerlis, *Phys. Rev. A* **86**, 053603 (2012), arXiv:1205.4815 [cond-mat.quant-gas].
- [28] M. M. Forbes and R. Sharma, “Validating simple dynamical simulations of the unitary fermi gas,” arXiv:1308.4387 [cond-mat.quant-gas].
- [29] Q. Chen, C. R. Howell, T. S. Carman, W. R. Gibbs, B. F. Gibson, A. Hussein, M. R. Kiser, G. Mertens, C. F. Moore, C. Morris, A. Obst, E. Pasyuk, C. D. Roper, F. Salinas, H. R. Setze, I. Slaus, S. Sterbenz, W. Tornow, R. L. Walter, C. R. Whiteley, and M. Whittom, *Phys. Rev. C* **77**, 054002 (2008).
- [30] C. J. Pethick and H. Smith, *Bose-Einstein Condensation in Dilute Gases* (Cambridge University Press, Cambridge, 2002).
- [31] L. Thompson and P. C. E. Stamp, *Phys. Rev. Lett.* **108**, 184501 (2012), arXiv:1110.6386.
- [32] D. J. Thouless and J. R. Anglin, *Phys. Rev. Lett.* **99**, 105301 (2007), arXiv:cond-mat/0703523.
- [33] W. F. Vinen and J. J. Niemela, *J. Low Temp. Phys.* **128**, 167 (2002).
- [34] P. Magierski and A. Bulgac, *Nucl. Phys. A* **738**, 143 (2004); *Acta Phys. Pol. B* **35**, 1203 (2004), arXiv:astro-ph/0312644.
- [35] A. Pfitzner, W. Cassing, and A. Peter, *Nucl. Phys. A* **577**, 753 (1994), arXiv:nucl-th/9404020.
- [36] A. Bulgac, M. M. Forbes, K. J. Roche, and G. Wlazłowski, “Quantum Friction: Cooling Quantum Systems with Unitary Time Evolution,” (2013), arXiv:1305.6891 [nucl-th].